Evolution of the frequency–spatial structure of an intense laser pulse propagating in a resonant medium

A. N. Starostin and A. A. Panteleev

Troitsk Institute for Innovative and Thermonuclear Studies, 142092 Troitsk, Moscow Province, Russia

V. I. Lebedev and S. V. Rotin

Russian Scientific Center "Kurchatov Institute," 123182 Moscow, Russia

A. G. Leonov and D. I. Chekhov

Moscow Physico-Technical Institute, 111700 Dolgoprudnyĭ, Moscow Province, Russia

(Submitted 11 May 1995)
Zh. Éksp. Teor. Fiz. **108**, 1203–1222 (October 1995)

The development of the spectral–angular instability of an intense laser pulse in an extended resonant absorbing medium is investigated within the framework of the Maxwell–Bloch equations. By means of numerical analysis we show here for the first time that for a shift of the laser frequency in either direction from the resonant transition the given model provides a good description of all of the main experimentally observable spatial and frequency characteristics of laser beams scattered in a resonant medium. Based on our model calculations of the propagation of a laser pulse in an amplifying resonant medium, we show that the pulse experiences an instability analogous to the spectral–angular instability it experiences in an absorbing medium. © *1995 American Institute of Physics.*

1. INTRODUCTION

Investigations of various types of instabilities accompanying the propagation of intense laser radiation in resonant media are among the most urgent problems in nonlinear optics. One of the best known of these is the spectral–angular instability of laser beams propagating in resonant gaseous media (see, e.g., Refs. 1 and 2 and the references therein). Experimental studies in this area have shown that in the case of a high-frequency detuning $\Delta=\omega_0-\omega_L<0$ of the laser frequency ω_L from the frequency of the atomic transition ω_0 the laser beam undergoes both a small-scale spatial instability, manifested in the breakup of the beam into separate self-focusing filaments, and a large-scale instability, manifested as conical emission. It is characteristic of this instability that the observed spectrum of the scattered radiation contains a number of components frequency-shifted from ω_0, the wavelengths and intensities of which depend in a complicated way on the scattering angle. In particular, the conical emission spectrum mainly contains a component that is significantly shifted toward the red from the frequency of the exciting laser beam. As was theoretically predicted in Ref. 3 and later confirmed experimentally in Refs. 4 and 5, an analogous, pronounced instability can also take place for $\Delta>0$.

To explain the origin of this instability, in particular the conical emission, a number of qualitative theoretical models have been proposed (reviews are given in Refs. 1 and 2): nondegenerate four-wave mixing (NFWM) with refraction of the shifted component at the boundary of the self-length focusing filament, NFWM under conditions of longitudinal wave synchronism, generation of Cherenkov radiation, downconversion, etc. However, they explain only separate aspects of this complicated problem and not one of them describes the entire manifold of experimental data. In this regard, as our experiments and their theoretical analysis[4,5] have shown, the most adequate description of the onset of the instability is provided by the NFWM model,[6,7] without resort to additional considerations. However, if the pump wave is assumed given, as in Refs. 4 and 5, it describes only the linear stage of the instability: its growth rate determines only the possible spectral regions of amplification of the satellites and their angular distribution. It should also be pointed out that in recent numerical calculations of NFWM processes[8] good agreement was obtained between theory and experiment in the stationary case for low intensities. Partial qualitative confirmation of the observed effects was obtained in Ref. 1 by numerically modeling the time dependent case. An interesting observation was made in Ref. 1, namely that the spatially inhomogeneous distribution of the pulse when it enters the medium creates a quasiperiodic spatial and temporal modulation of the polarization, which in turn can serve as a trigger for the onset of the small-scale instability even for a smooth initial profile. However, only the case $\Delta<0$ was calculated in Refs. 1 and 8; in Ref. 1 the calculations were carried out for a conservative system (i.e., relaxation processes were not taken into account) and short propagation lengths of the pulse, L, so that the instability did not become fully developed.

Note that the majority of experimental studies of propagation of intense (powers around 1 MW/cm^2 and greater) laser radiation in resonant gaseous media have had a substantially time-dependent character: the laser pulse was of the order or shorter than the characteristic relaxation time of the atomic subsystem. Earlier theoretical studies, including numerical, of the evolution of time-dependent, intense electromagnetic radiation in resonant media, besides Ref. 1, have mainly addressed 2π-pulses. Bol'shov *et al.*[9–11] showed that

 1063-7761/95/100660-11$10.00

2π-pulses in a two-level medium experience a transverse instability for either sign of the detuning. We point out that the analytic studies of the growth rates of this instability[9,10] were performed only for spectrally degenerate modes. Numerical calculations were performed in Ref. 11, for the case of exact resonance of the carrier frequency of the 2π-pulse with the transition frequency, which confirmed the presence of this instability. However, the calculations in Ref. 11 did not describe the fully developed instability.

In the present paper we present a numerical time-dependent analysis of propagation of an intense laser pulse in a resonant—and, in contrast to Ref. 1, extended and absorbing—medium. Our analysis describes the nonlinear stage of the development of the instability and explains for the first time all the key experimental data, both those obtained earlier for $\Delta<0$ and those obtained in Refs. 4 and 5 for $\Delta>0$: the development of the small-scale instability, the generation of one or several cones of radiation and their spectral makeup, significant spatial and frequency broadening of the spectral components of the scattering, etc. We also examine the spectral–angular instability of a laser pulse propagating in an amplifying two-level medium.

2. THEORY

We study the evolution of an intense laser pulse propagating in a gas of two-level atoms. To describe the intensity of the total radiation field $E(z,r_\perp,t)$ in the medium we may use Maxwell's equation in the parabolic approximation of Langevin:

$$\left(\frac{1}{c}\frac{\partial}{\partial t}+\frac{\partial}{\partial z}-\frac{i}{2k_L}\Delta_\perp\right)E(z,r_\perp,t)$$
$$=i\frac{2\pi\omega_L}{c}N\mu_{12}\rho_{21}+F^{st}(z,r_\perp,t),$$
$$\Delta_\perp=\frac{\partial^2}{\partial x^2}+\frac{\partial^2}{\partial y^2},\quad (t,r_\perp)\in R^3,\quad r_\perp=(x,y), \tag{1}$$
$$z\in[0,L].$$

Here k_L is the wave vector of the laser wave.

The first term on the right-hand side of this equation describes induced processes associated with the interaction of the radiation with the medium. The polarization induced in the medium is found by solving the equations for the components ρ_{jk} $(j,k=1,2)$ of the density matrix of the two-level atom:

$$i\frac{\partial}{\partial t}\rho_{22}=V\rho_{12}-\rho_{21}V^*-i\gamma_1\rho_{22},\quad \rho_{11}+\rho_{22}=1,$$
$$i\frac{\partial}{\partial t}\rho_{21}=V(\rho_{11}-\rho_{22})-i\gamma_2\rho_{21},\quad \rho_{12}=\rho_{21}^*, \tag{2}$$

where $V=-\mu_{21}E/2\hbar$, μ_{21} is the matrix element of the dipole moment, γ_1 and γ_2 are the longitudinal and transverse relaxation rates of the two-level atoms with density N. Equation (2), for convenience of the numerical calculations, uses a modification of the rotating wave approximation: the energy of the photons of the radiation field is counted from the energy of the atomic transition.

The second term F^{st} on the right-hand side of Eq. 1 describes the contribution due to spontaneous emission of the atoms. The most convenient way to calculate F^{st} with allowance for spontaneous emission is to use the formalism of the atom–photon density matrix,[12] which was first used to calculate resonant fluorescence spectra by Baklanov.[13] For stationary fields this method has been substantially developed by Sargent and coworkers (see Ref. 14).

In the present paper we assume that the field strength of the laser pulse entering the medium has a Gaussian distribution in the transverse spatial coordinate and in time:

$$E_L|_{z=0}=E_0\exp\left(-\frac{r_\perp^2}{2a^2}-\frac{t^2}{2t_p^2}-it\Delta\right), \tag{3}$$

where $2a$ is the transverse diameter of the beam, and $2t_p$ is the duration of the pulse.

Note that in the stationary regime (or for very long pulses) system of equations (1), (2) can be transformed into a system of equations for the laser wave and a set of symmetrically detuned coupled modes E_j satisfying the wave synchronism condition:

$$\left(\frac{\partial}{\partial z}-\frac{i}{2k_L}\Delta_\perp\right)E_L=a_LE_L, \tag{4}$$

$$\left(\frac{\partial}{\partial z}-\frac{i}{2k_L}\Delta_\perp\right)E_j=\alpha_jE_j+\beta_jE_{j'}+F_j, \tag{5}$$

$$\left(\frac{\partial}{\partial z}-\frac{i}{2k_L}\Delta_\perp\right)E_{j'}^*=\alpha_{j'}^*E_{j'}^*+\beta_{j'}^*E_j+F_{j'}^*; \tag{6}$$

under the condition

$$\omega_j+\omega_{j'}=2\omega_L,\quad \mathbf{k}_j+\mathbf{k}_{j'}\approx 2\mathbf{k}_L. \tag{7}$$

The coefficients α_j and β_j are found from Eqs. (2), where the total field E is defined as

$$E=E_L+\sum_j E_j. \tag{8}$$

For weak depletion of the pump wave $E_L\gg\Sigma_jE_j$, the coefficients α_j and β_j can be calculated from perturbation theory and are described by the expressions for the absorption (gain) coefficients of the probe signal and four-wave mode coupling (see Refs. 7 and 15). Here, assuming spatial and temporal δ-correlation of the quantities F_j, the following relations hold:

$$\langle F_jE_{j''}^*\rangle\propto A_j\delta_{jj''}, \tag{9}$$

$$\langle F_jE_{j''}\rangle\propto C_j\delta_{j''j'}, \tag{10}$$

where $\delta_{jj''}$ and $\delta_{j''j'}$ are Kronecker symbols, where the modes with indices j and j' are related by condition (7). The quantity A_j describes the resonant fluorescence spectrum of a two-level atom,[13,16] and C_j is the spontaneous source for the correlator $\langle E_j\ E_{j'}\rangle$ (Ref. 17).

Note that good agreement between theory and experiment in the description of the conical emission was first ob-

tained in Ref. 8 by numerical solution of system of equations (4)–(6). It also bears pointing out that this same system of equations, but without the assumption of spatial δ-correlatedness in relations (9) and (10), was investigated in Ref. 2, where it was shown that propagation of intense laser radiation in a resonant medium can be accompanied by generation of Cherenkov radiation.

In the present paper we carry out a numerical study of the propagation of a laser pulse for an amplifying and absorbing two-level media. The calculations were carried out for short pulses ($t_p \ll \gamma_1^{-1}$, γ_2^{-1}). In this case it is possible to neglect the effect of spontaneous emission and drop the term F^{st} in Eq. (1), which substantially simplifies the calculations.

3. NUMERICAL MODEL

Equations (1) (without the term F^{st}) and (2) form the well-known system of Maxwell–Bloch equations. For convenience in the numerical model, we put them in dimensionless form. Transforming first to the retarded time $t' = t - z/c$, we obtain the following equations:

$$\frac{\partial \rho_1}{\partial \tau} = -G\ \mathrm{Re}(e\rho_2^*) - \Gamma_1 \rho_1, \tag{11a}$$

$$\frac{\partial \rho_2}{\partial \tau} = -Ge\left(\rho_1 - \frac{1}{2}\right) - \Gamma_2 \rho_2, \tag{11b}$$

$$\left[\frac{\partial}{\partial \zeta} - i\Phi\Delta_\xi\right] e = M\rho_2, \tag{12}$$

where

$$\Delta_\xi = \frac{\partial^2}{\partial \xi_x^2} + \frac{\partial^2}{\partial \xi_y^2}, \quad \xi = (\xi_x; y), \quad (\tau, \xi) \in \mathrm{R}^3,$$

$$\zeta \in [0; \zeta_k].$$

Here for the absorbing medium

$$\rho_1|_{t \to -\infty} = \rho_2|_{t \to -\infty} = 0, \tag{13a}$$

and for an inverted medium

$$\rho_1|_{t \to -\infty} = 1, \quad \rho_2|_{t \to -\infty} = 0. \tag{13b}$$

The boundary conditions on the pulse as it enters the medium have the form

$$e|_{\zeta=0} = \exp\left(-\frac{\xi^2}{2} - \frac{\tau^2}{2} - i\delta^0\tau\right) + \sum_{s \geqslant 1} A_s \exp[i(\sigma^s \xi - \delta^s \tau)], \tag{14}$$

where the first term describes the laser pulse, and the sum describes the set of low-intensity noise harmonics which are introduced to investigate the influence of noise triggers (the role of spontaneous emission) on the propagation of the pulse. The dimensionless quantities in expressions (11)–(14) are defined as follows:

$$E = E_0 e, \quad \|\rho_{ij}\| = \begin{Vmatrix} 1-\rho_1 & i\rho_2 \\ -i\rho_2 & \rho_1 \end{Vmatrix}, \quad \tau = \frac{t'}{t_p},$$

$$\xi_x = \frac{x}{a}, \quad \xi_y = \frac{y}{a}, \quad \zeta = \frac{z}{ct_p},$$

$$G = \mu t_p E_0/\hbar, \quad \Gamma_i = \gamma_i t_p, \quad \Phi = \frac{t_p c}{2a^2 k_L},$$

$$M = 4\pi\omega_0 t_p \left(\frac{N\mu}{E_0}\right), \quad \delta^s = \Delta^s t_p,$$

$$\sigma^s = \kappa^s a, \quad A_s = E_s/E_0,$$

where E_s is the field strength of the sth mode of the noise triggers, and Δ^s and κ^s are its detuning from resonance and the transverse component of the wave vector, respectively.

The system (11), (12) is evolutionary in both the variables τ and ζ, and can be represented as a composition of a time problem [Eq. (11), where e is a known function] and a depth problem [Eq. (12), where ρ_2 is a known function]. Each of these problems requires the development and application of specific numerical methods.

In the given calculations the grid in the space (τ, ξ, ζ) was taken to be nonuniform-rectangular. The following sequence of values of the grid functions corresponding to the unknown fields ρ_1, ρ_2, and e was used. First the time problem is solved numerically at a fixed depth for which values of the function e^h at the grid-points are already known and are interpolated over the entire time axis with the help of a local cubic spline.[18] Then, after calculating ρ_1^h and ρ_2^h at this same depth, a global step is made in ζ. At the same time, ρ_2 on the right-hand side of Eq. (12) is calculated using a special third-order interpolator constructed from the layers already calculated. As the end result, only the final layer remains in memory: $\rho_1(\tau, \xi, \zeta_k)$, $\rho_2(\tau, \xi, \zeta_k)$, and $e(\tau, \xi, \zeta_k)$, characterizing the readings of the sensors located at the depth ζ_k.

The solution of problem (11), (13) in time is realized with the help of a software package called DUMKA which implements stable explicit difference schemes with variable steps in τ for systems of rigid homogeneous differential equations.[19] The time steps are determined by a special algorithm which takes account of the characteristics of the spectrum of the problem and ensures an accelerated step in comparison with classical schemes. To solve the problem (12), (14), we used special difference schemes of Crank–Nicolson type (in ζ),[20] in which, to obtain a high order of accuracy ($O(h^4)$), two positive steps were cyclically multiplied with one negative step. The equations arising in this manner were solved by five-point multiple-pass methods. Besides the methods above indicated, we may distinguish the three most important parts of the calculational section of the software package:

a) use of adaptive grids in the transverse layer (ξ) and in time (ζ, τ);

b) interpolation of the right-hand side of Eq. (12) in sparse regions of the grid;

c) an algorithm for choosing the variable step in depth, which ensures a constant local error ~2–3% in the solution.

These algorithms and methods allowed us not only to substantially shorten (by several orders of magnitude) the run time of the calculations in comparison with standard

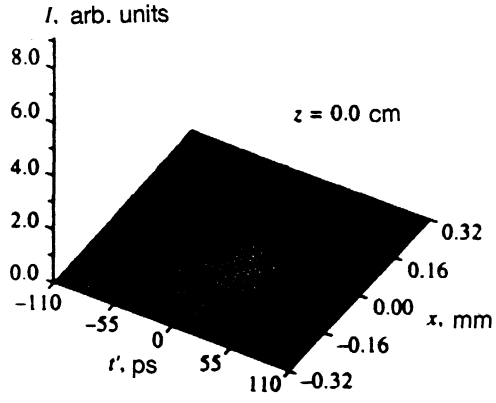

FIG. 1. Shape of the laser pulse as it enters the medium.

methods for solving problems of the given type,[1,8] but also to significantly broaden the region of permissible values of the parameters. Moreover, the numerical modeling in Refs. 1 and 8 was performed on powerful Cray computers, whereas the calculations in the present paper were carried out on a PC DX2-486.

4. NUMERICAL RESULTS

A. Pulse propagation in an absorbing medium

Here we will present results of our calculations of the evolution of a laser pulse of duration $2t_p=0.1$ ns and intensity $I=0.64$ W/cm^2, entering the medium with the shape shown in Fig. 1. Figures 2–7 present the results of two-dimensional (with one transverse coordinate) calculations of the modification of the space-time and frequency–angular characteristics of the laser pulse as it propagates along the z axis in absorbing media [initial conditions (13a)] with resonant particle density $N=1.7\cdot 10^{14}$ cm^{-3} for two symmetric laser detunings $\Delta=\pm 48$ GHz and with the lower density $N=4.1\cdot 10^{13}$ cm^{-3} at exact resonance $\Delta=0$, which is associated with significantly larger absorption in this case. The atomic transition parameters in the calculations were taken to be those of the $D2$ line of sodium ($\lambda=588.995$ nm), $\gamma_2=5\gamma_1=5\gamma$ (γ is the radiative relaxation rate). The choice of a relatively short pulse was determined by the limitations of the computer, on which a reasonable calculation time was determined by the condition $Vt_p<10^3$.

The calculations of the space-time evolution of the laser pulse (see Figs. 2 and 3) show that in the initial stage of propagation in a resonant medium the pulse breaks up into 2π-pulses, resulting in the formation of several regular large-scale solitons. Note that the formation of a multisoliton structure in the propagation of short pulses in a resonant medium is well known and associated with the phenomenon of self-induced transparency.[21]

We introduce, following Ref. 21, the dimensionless area of the pulse

$$\int \Omega(t)\,dt=2\pi n, \tag{15}$$

where $\Omega(t)=2V(t)$ is the Rabi frequency. For the given values of the pulse parameters and of the medium itself, n is approximately equal to 10. This value is in agreement with the results of calculations at the depth $z=0.75$ cm (see Figs. 2 and 3), where nine peaks are distinctly revealed along the axis of the pulse, independent of the sign of the detuning. Note that as the laser pulse propagates, it is observed to slow down, this being a characteristic property of 2π-pulses. Our results are in agreement with the calculations of Ref. 1, which were restricted to moderate depths.

In the present calculations we have succeeded in tracing the space-time evolution of the shape of the pulse to a significantly later stage. It is found that as the pulse propagates into the resonant medium, the large-scale regular soliton structure gradually washes out and is replaced by numerous small-scale formations (see Fig. 2, $z=3$ cm and Fig. 4). It is particularly important that, as can be seen from Figs. 2 and 4 (see also Figs. 5–7), at large depths the small-scale instability (filament formation) is observed not only at $\Delta<0$, but contrary to the generally accepted degenerate instability model of Bespalov–Talanov[22] (a partial case of which for a resonant medium is the Javan–Kelley instability[23]) also for $\Delta>0$, which confirms the conclusions of the theory developed in Ref. 3 and is in line with the experimental observation of this effect in Refs. 4 and 5. Linear analysis[3–5] shows that this instability is due to NFWM.

The spectral–angular structure of the scattered laser beam, obtained by taking the Fourier transform of its space-

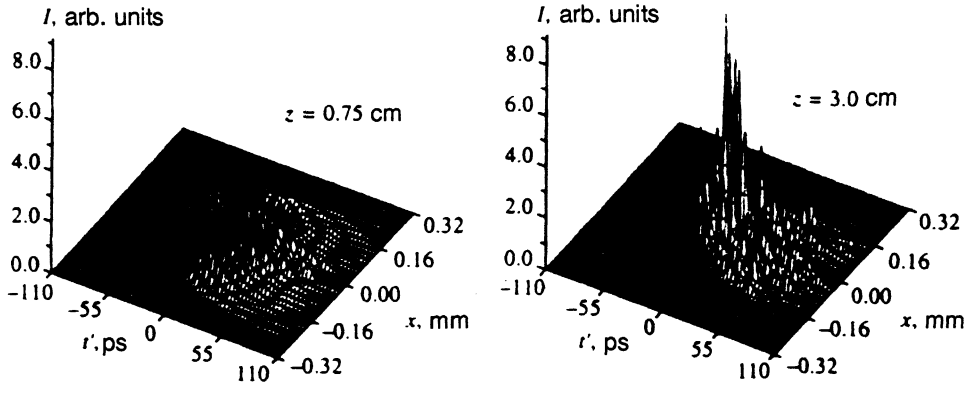

FIG. 2. Modification of the space-time structure of a laser pulse as it propagates in a resonant medium for $I=0.64$ MW/cm^2, $2t_p=0.1$ ns, $N=1.7\cdot 10^{14}$ cm^{-3}, and $\Delta=0$.

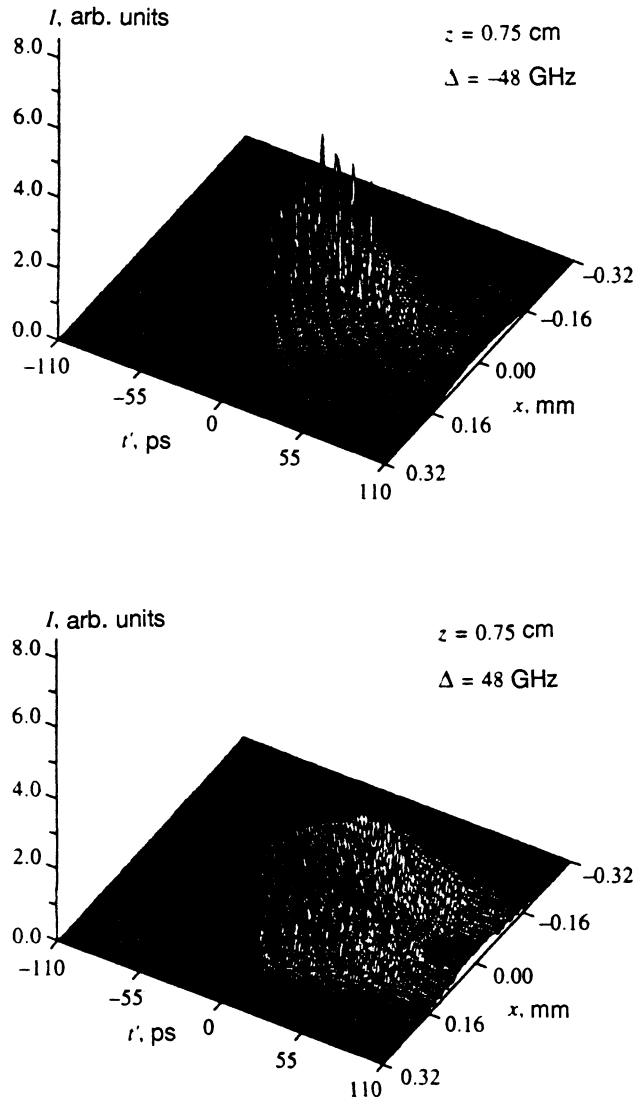

FIG. 3. Modification of the space-time structure of a laser pulse as it propagates in a resonant medium for $\Delta = \pm 48$ GHz, (other parameters as in Fig. 2).

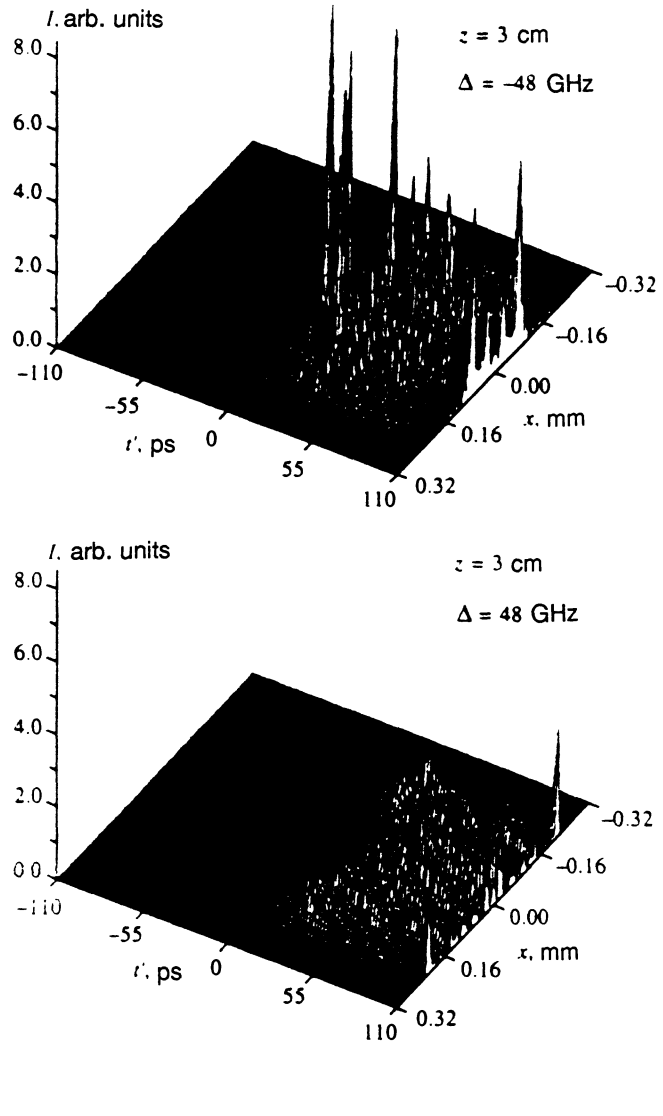

FIG. 4. Modification of the space-time structure of a laser pulse as it propagates in a resonant medium for $\Delta = \pm 48$ GHz, (other parameters as in Fig. 2).

time structure, is shown in Figs. 5–7. It follows from Fig. 5 that for detuning $\Delta < 0$ the spectral–angular characteristics of the laser beam undergo substantial modification even at $z = 0.75$ cm, as evidenced by the significant spatial and frequency broadening of the spectrum of the exciting laser radiation, and also by the appearance of two scattering components frequency-shifted relative to ω_L. Note that in this case the red component has a broad angular distribution, whereas the blue propagates along the axis of the laser beam, and what is important, agrees with the experimental results (see, e.g., Refs. 24 and 25). Next, it is clear from Fig. 5 that as the laser beam continues its advance into the medium the red component forms the conical emission, whereas the laser line and the blue component overlap, forming a single line broadened both in frequency and in angle (see Fig. 5, $z = 3$ cm. Here it should be noted that both shifted scattering components were previously observed experimentally[24] at moderate density $N \sim 10^{14}$ cm^{-3} and short resonant medium. At the same time, the absence in the scattering spectrum of a spectrally distinct blue component at higher densities of the medium corresponding to significantly longer interaction lengths (as has in fact been experimentally observed in a number of works[24,26,27]), was the reason given in Ref. 28 for considering the Cherenkov effect (which does not require, as does NFWM, that the Manley–Rowe relations hold) as a possible reason for the appearance of conical emission for $\Delta < 0$. For a more concrete comparison of the calculated results with the experimental data, Fig. 8 shows spectra, which we measured under interaction conditions close to those calculated, of the radiation scattered at different angles in a resonant medium of sodium vapor for $\omega_L > \omega_{D2}$, where ω_{D2} is the frequency of the resonant $D2$ sodium line. (A detailed description of the measurement technique can be found in Refs. 4 and 5.) Comparison of the data presented in Fig. 5 ($z = 3$ cm) and 8 shows that at large depths the numerical model provides a good qualitative description of all the experimentally observed behavior.

As has already been mentioned, the numerical analysis

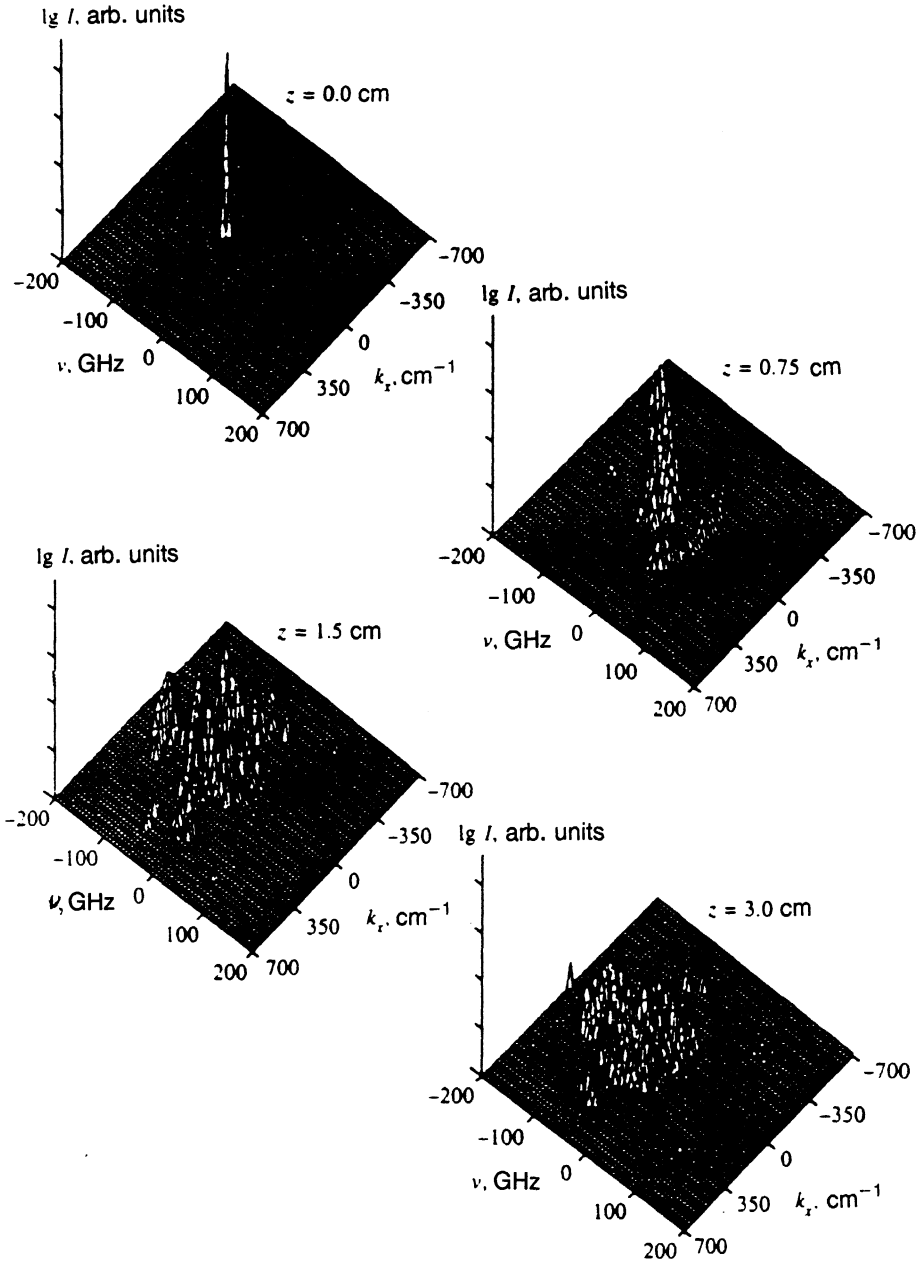

FIG. 5. Modification of the frequency–angular structure of a laser pulse as it propagates in a resonant medium for $\Delta = -48$ GHz (other parameters as in Fig. 2).

of the laser beam propagation instability relates to the short pulse regime ($t_p \ll \gamma_2^{-1}$, γ_1^{-1}). On the other hand, in our experiments and in the overwhelming majority of other experimental studies the pulse satisfied the condition $\gamma_1^{-1} \ll t_p \sim \gamma_2^{-1}$, for which reason comparison with the experimental data can give cause for objection. However, experimental data are also known which correspond to the short pulse regime which we calculated[29,30] and which show that all of the main regularities present in the propagation of long pulses are also manifested in this case. This confirms the assertion that the fundamental mechanisms leading to the spectral–angular instability of laser radiation are identical for both short and long pulses (and even continuous radiation[8,31]).

Calculations carried out for $\Delta > 0$ (Fig. 6) show that the scattering picture as a whole is analogous to the case $\Delta < 0$. Specifically, in the initial stage of pulse propagation a red as well as a blue scattering component appears, both broadening in frequency and spatially with increasing z. Note that at large depths z for both $\Delta < 0$ and $\Delta > 0$ the spectrum of the laser radiation turns out to be preferentially frequency-broadened toward the side opposite the resonance, which is in agreement with experiment.[4,5,24] However, in contrast to the case $\Delta < 0$, for low-frequency laser detunings the rescattered radiation has a broader and less contrasted angular distribution and a somewhat narrower spectral composition (see Figs. 5 and 6, $z = 3$ cm), which also is in agreement with the experimental data[5]. Under conditions of exact resonance the instability is somewhat less pronounced due to the large absorption even at lower densities (see Fig. 7), but its spectral–angular characteristics are modified just as much with propagation of the pulse as in the presence of significant detuning.

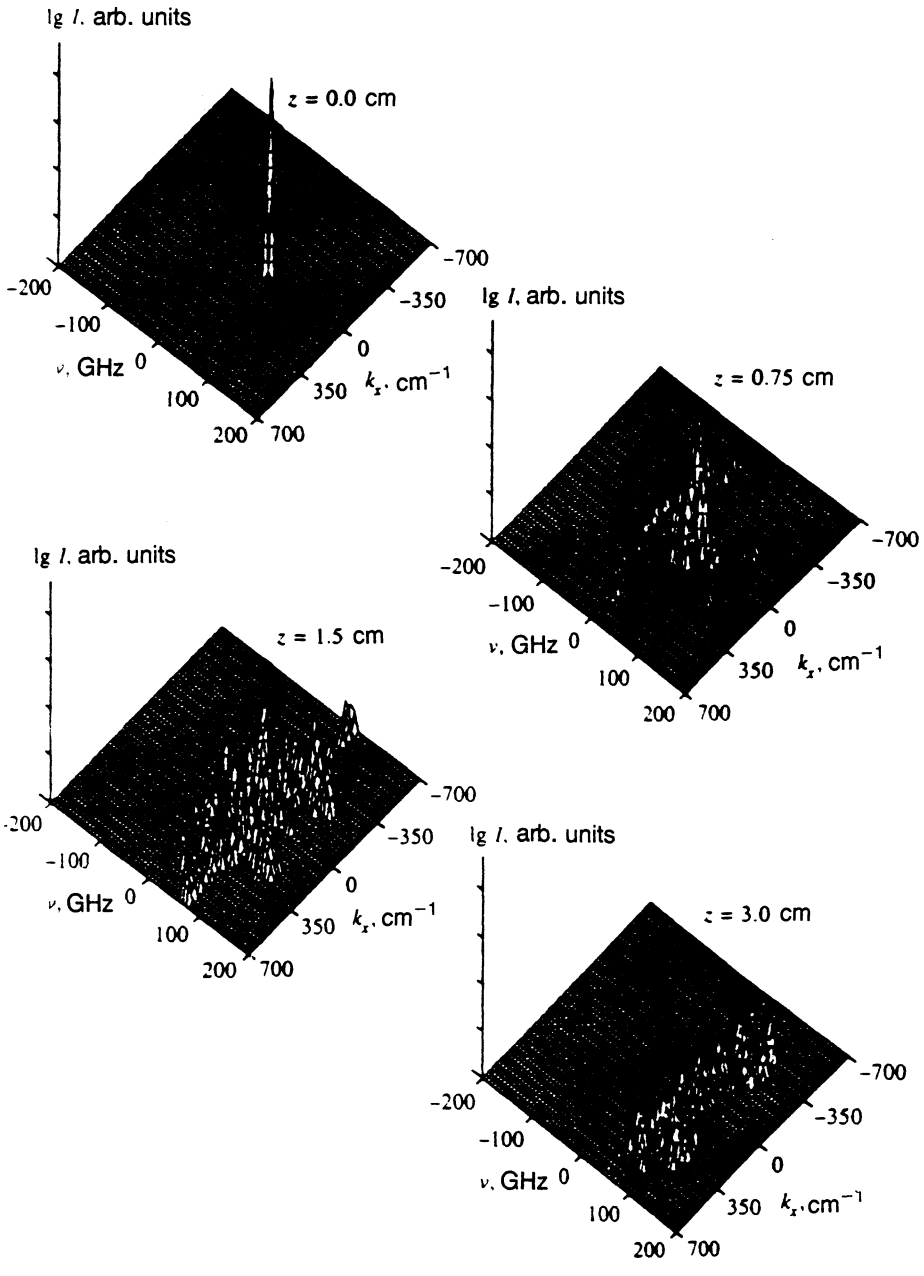

FIG. 6. Modification of the frequency–angular structure of a laser pulse as it propagates in a resonant medium for $\Delta = 48$ GHz(other parameters as in Fig. 2).

Note that both for $\Delta<0$ and for $\Delta>0$ the spectral widths of the individual components narrow down with increasing scattering angle, as was indicated in the linear analysis and was observed experimentally.[4,5]

Time-integration of the spatial profiles of the scattered laser beam at large depth $z=3$ cm show (Fig. 8) that for both $\Delta<0$ and $\Delta>0$ several rings are formed in the cross section of the laser beam, which was also observed in our experiments (see Fig. 9 for the case $\omega_L>\omega_{D2}$). The multiring structure was observed in Refs. 4, 5, and 25 for $\omega_L<\omega_{D1}$. Note that spatial self-modulation of the laser beam due to its transverse inhomogeneity affects the formation of the large-scale ring structure, as has been indicated for spectrally degenerate radiation in many papers (see, e.g., Refs. 32 and 33). In our calculations the regular transverse structure is clearly visible at small z (see Figs. 2 and 3). However, the complicated frequency–angular structure arising at large depths (which is especially well pronounced in experiments with blue detuning and which has acquired the name "conical emission" in the literature) is a consequence of the superposition of two primary effects: spatial self-modulation and the nondegenerate four-wave instability, whereby the latter gives rise to breakup into small-scale filaments even for a smooth pulse.

The calculations presented in Figs. 1–7 do not take account of any trigger noise fields in the system of equations, i.e., the coefficients A_s are set equal to zero in boundary condition (14). In this regard it should be noted that, as was shown in Ref. 1, for spectrally nondegenerate modes $\omega \neq \omega_L$ to appear in the interaction of the laser pulse with the medium noise fields need not be present, since trigger radiation in the modes whose frequencies are shifted relative to the laser frequency arises independently, thanks to self-modulation of the initial pulse upon entrance to the medium.

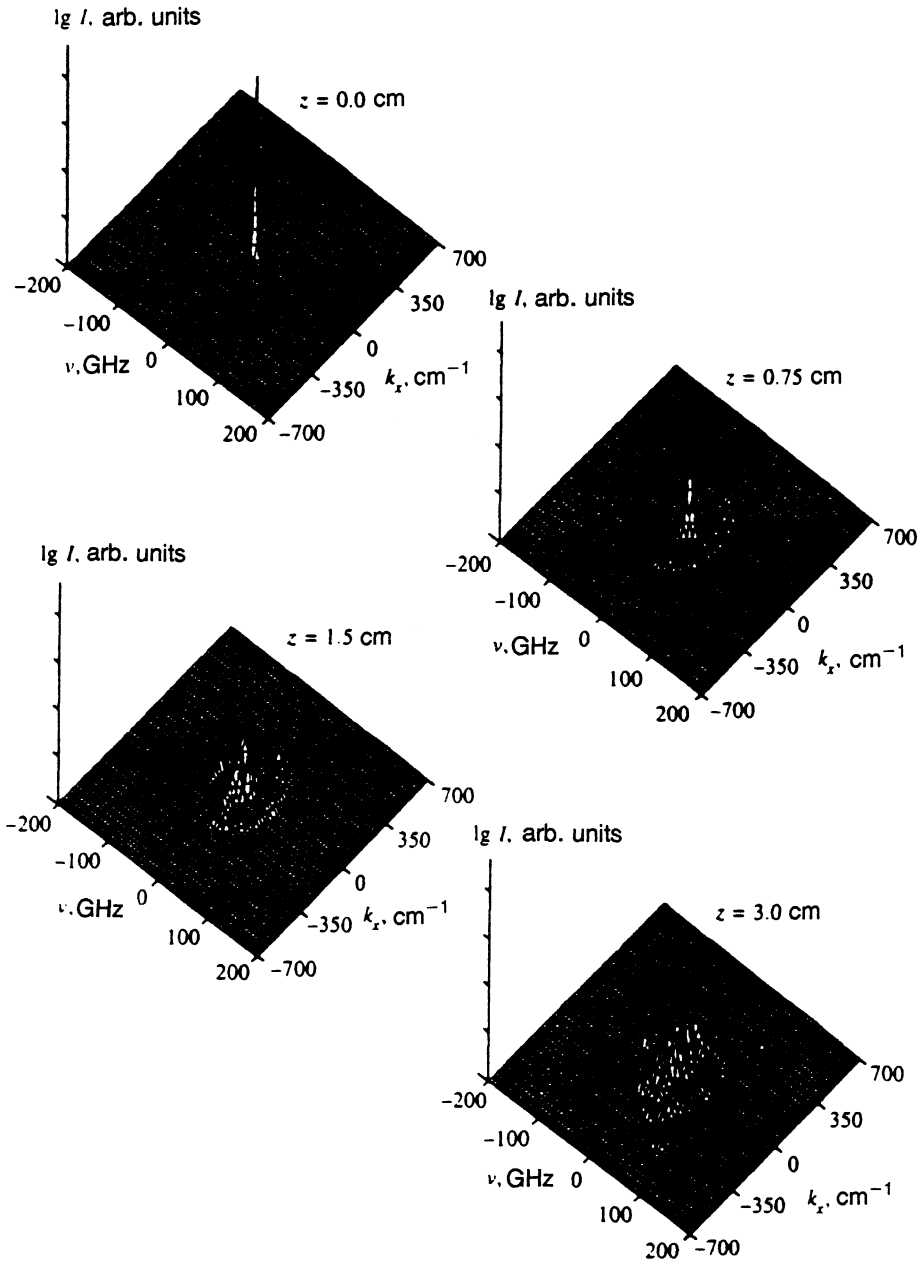

FIG. 7. Modification of the frequency–angular structure of a laser pulse as it propagates in a resonant medium (interaction parameters as in Fig. 2).

However, for a more detailed check of the influence of spontaneous sources [the last term in expression (1)], we carried out calculations with trigger noise fields with frequencies lying near the presumed maxima of the resonant fluorescence spectrum, and with intensities $I_s \sim A_s A_s^*$ reaching $0.01 I_0$. As the results of these calculations show, such noise fields have no substantial effect on the overall scattering pattern in the developed instability regime.

B. Pulse propagation in an amplifying medium

As was already mentioned, in addition to propagation of a laser pulse in an absorbing resonant medium, we have also investigated the stability of the passage of a pulse in an inverted amplifying medium, i.e., in a medium in which the initial conditions correspond to Eq. (13b). We carried out model calculations under exact resonance conditions for the

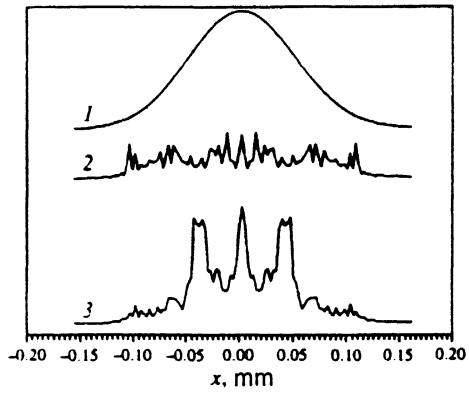

FIG. 8. Transverse distribution of the laser pulse as it enters the medium (curve *1*) and as it leaves it for $\Delta = 48$ GHz (curve *2*) and for $\Delta = -48$ GHz (curve *3*). The remaining interaction parameters are as in Fig. 2.

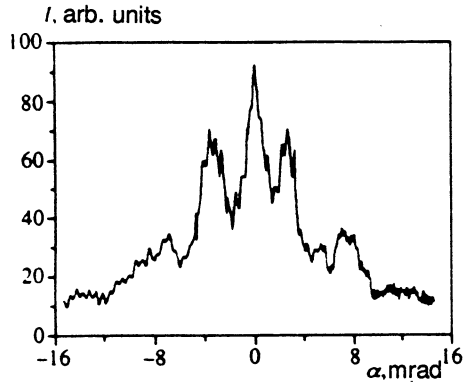

FIG. 9. Experimentally measured angular distribution of the exit radiation for the parameters as in Fig. 6.

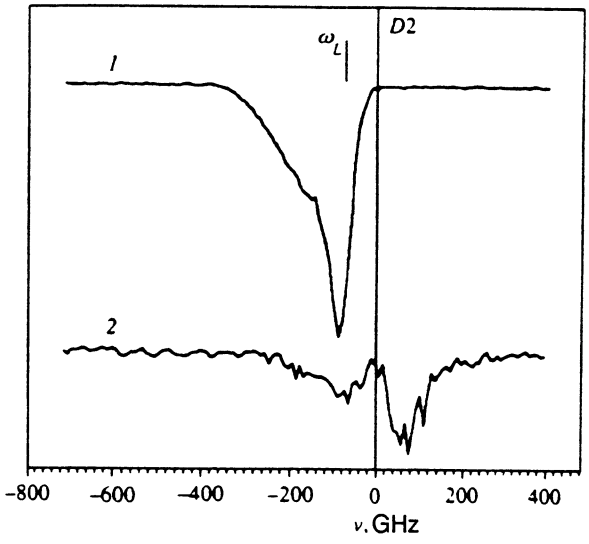

FIG. 10. Experimentally measured characteristics of the spectral distribution of the exit radiation, observing along the axis of the exiting beam (curve *1*) and at an angle of $\theta = 50$ mrad to it (curve *2*). The laser pulse as it entered the medium was detuned by $\Delta\nu = 80$ GHz toward the blue from the *D2* line of sodium and had an intensity of $I = 4$ MW/cm^2. The sodium vapor density was $N = 4 \cdot 10^{14}$ cm^{-3}.

following dimensionless parameter values of the pulse and the medium: $G = 15$, $\Phi = 0.01$, $M = 200$, and $\Gamma_{1,2} = 0.012$, the results of which are presented in Figs. 11–13.

As the results of our calculations show, in the initial stage one observes the usual saturated amplification and diffraction broadening of the pulse. At the entrance to the medium the pulse has low energy and $n \ll 1$, where the quantity n is defined by relation (15). In the saturated amplification regime, n grows as the pulse propagates ($n \sim z^{1/2}$) and after sufficient amplification, when n becomes greater than unity, the pulse breaks up, as in an absorbing medium, into solitons (see Fig. 11, $\zeta = 0.1$). As the pulse continues to propagate, a small-scale nondegenerate pulse instability appears (see Figs. 11 and 12). In the presence of a spectral–angular instability in the propagation of a monochromatic wave in a resonant amplifying medium, our calculated results back up our estimates using NFWM theory.[6,7] In the stationary case the

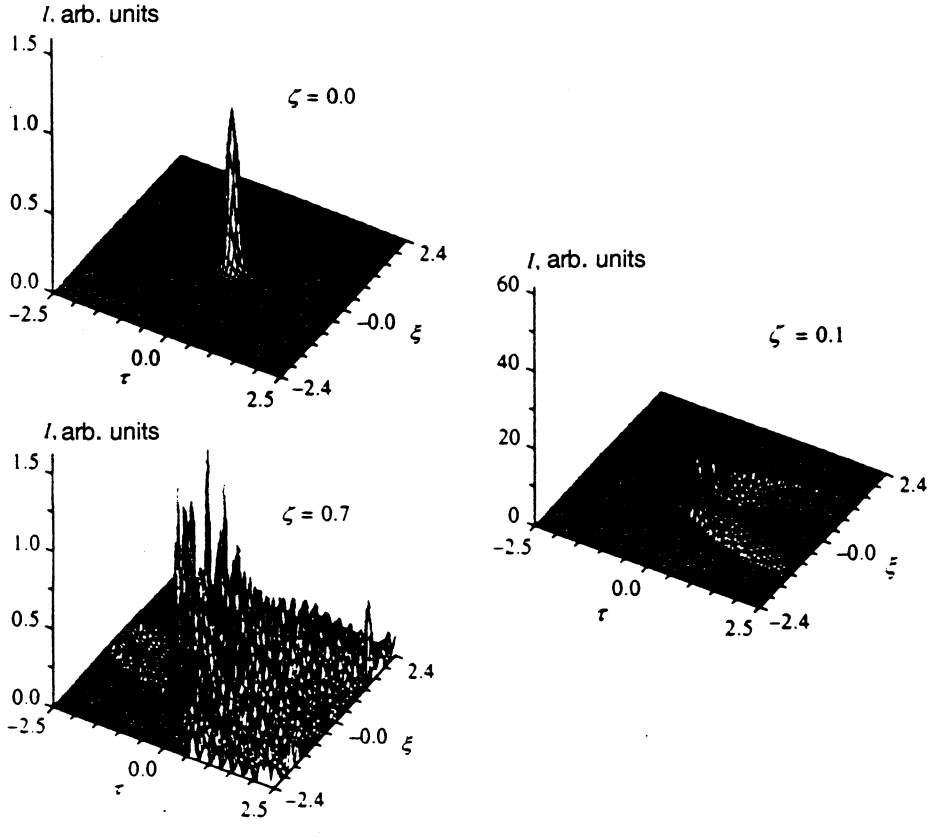

FIG. 11. Results of a calculation of the propagation of a laser pulse in an amplifying medium under conditions of exact resonance for $G = 15$, $\Phi = 0.01$, $M = 200$, and $\Gamma_{1,2} = 0.012$. For $\zeta = 0$ the scale of the intensity was increased by a factor of 40 relative to its value for $\zeta = 0.1$ and 0.7.

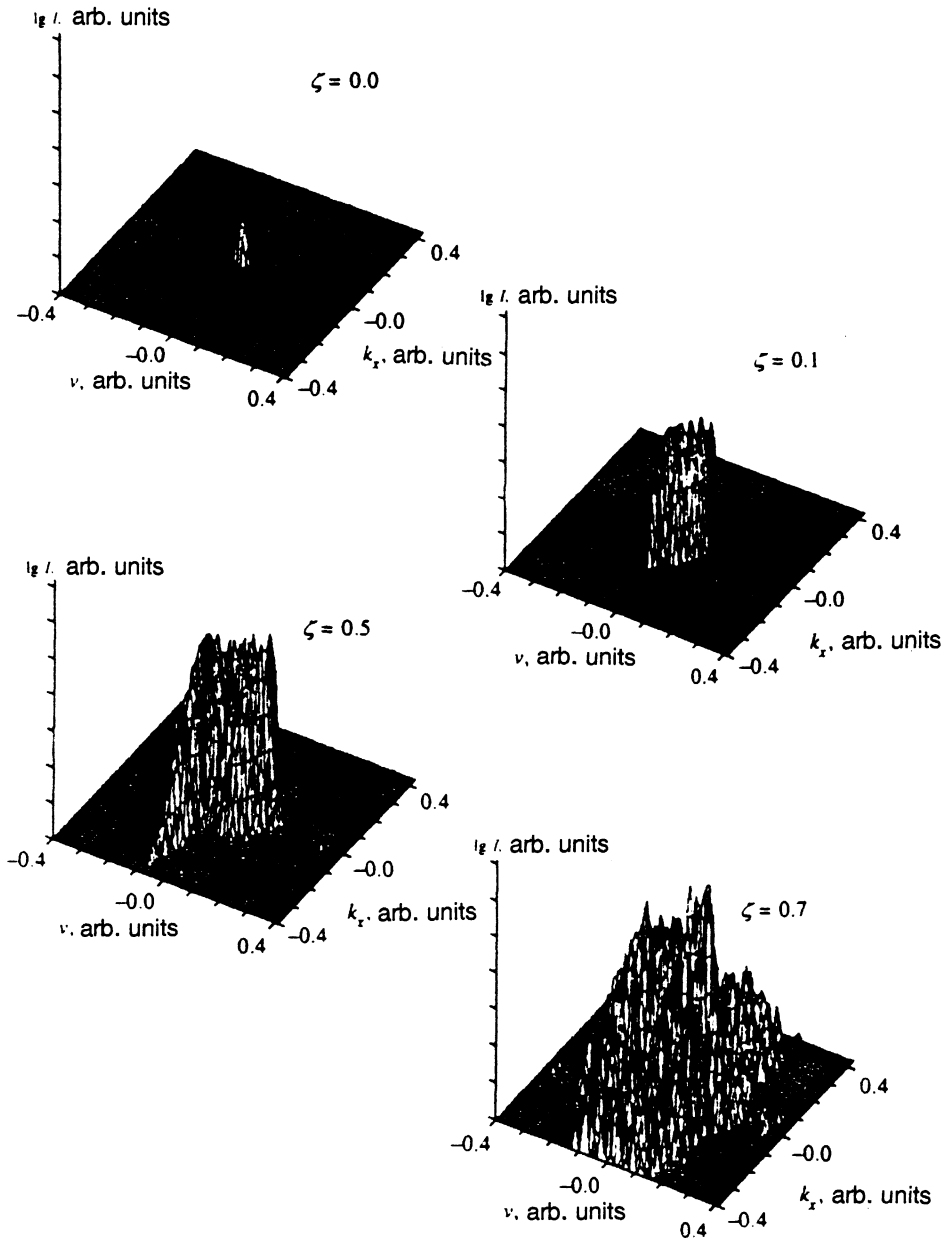

FIG. 12. Modification of the frequency–angular structure of a pulse propagating in an amplifying medium. The parameters are as in Fig. 11.

growth rate of the instability is proportional to $I^{-1/2}$, while it is well known that the gain coefficient of the medium is proportional to I^{-1} at saturation. One can expect this effect to occur also under nonstationary conditions. This means that small-scale perturbations will be amplified faster than the pulse as a whole, which can lead to substantial deterioration of the main characteristics of the laser pulse: its divergence, linewidth, etc. A substantial difference between the instability of a laser pulse in an amplifying medium from its instability in an absorbing medium is the constant growth of the radiation intensity. This leads to the result that despite large linear growth rates, the instability develops more slowly in an amplifying medium, since a significant change in the parameters of the laser pulse as it propagates significantly changes the spectral characteristics of the parametric processes and renders the conditions of wave synchronism nonoptimal.

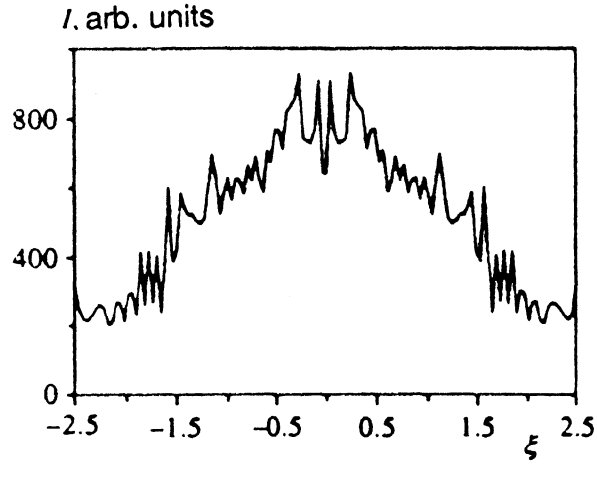

FIG. 13. Transverse distribution of a laser pulse propagating in an amplifying medium at a depth of $\zeta = 0.7$ for the same parameter values as in Fig. 11.

Integrating the spatial profiles of the amplified laser beam over time shows (see Fig. 13) that a multiring structure is also formed in the transverse distribution of the laser pulse. However, in contrast to the case of an absorbing medium, its contrast is substantially less. Note that formation of a ring structure was predicted in Ref. 34 for the degenerate stationary case of amplification of a Gaussian beam.

The calculated instability can manifest itself in laser amplifiers with large gain coefficients. Note that the small-scale instability frequently observed in experiments in neodymium-glass amplifiers may be substantial due to the resonance contribution n_2 to the nonlinear addition to the refractive index, whose magnitude can reach 85% (see, e.g., Ref. 35).

5. CONCLUSION

Our numerical calculations have established that intense short pulses propagating in a resonant medium undergo a spectral–angular instability for either sign of the resonance detuning. We have shown here for the first time that a model based on the Maxwell–Bloch system of equations without any additional or alternative mechanisms is sufficient to describe the developed stage of this instability. Note that experimental data are available which correspond to the fully developed instability regime and can be described by this model. Qualitatively, the results observed in experiment for $\Delta \gtrless 0$ find completely satisfactory confirmation within the framework of the proposed model.

Model calculations have been performed which describe the propagation of a short pulse in an amplifying medium. We have found that a substantially amplified pulse breaks down into soliton formations and experiences a spectral–angular instability. The proposed model can be used to analyze laser systems working in the amplification regime.

Finally, a numerical software package has been developed to solve the Maxwell–Bloch system of equations that allows one to efficiently solve problems of the given type, including three-dimensional problems if a sufficiently powerful computer is available.

ACKNOWLEDGMENTS

The present work was carried out with the support of the Russian Foundation for Fundamental Research (Grants No. 9-02-05853 and No. 93-01-00251) and the International Scientific Fund (Grant No. RLT 300). The authors also thank Yu. V. Petrushevich for discussion of results and A. N. Kazakov for providing computer programs for solving Eq. (12) by the five-point "multisweep" method.

[1] M. E. Grenshow and C. D. Cantrel, Phys. Rev. A **39**, 126 (1989).
[2] L. You, J. Mostowsky, and J. Cooper, Phys. Rev. A **46**, 2925 (1992).
[3] A. A. Panteleev, V. A. Roslyakov, A. N. Starostin, and M. D. Taran, Zh. Éksp. Teor. Fiz. **97**, 1777 (1990) [Sov. Phys. JETP **70**, 1003 (1990)].
[4] D. V. Gaĭdarenko, A. G. Leonov, A. A. Panteleev, V. A. Roslyakov, A. N. Starostin, and D. I. Chekhov, Pis'ma Zh. Éksp. Teor. Fiz. **55**, 229 (1992) [JETP Lett. (1992)].
[5] D. I. Chekhov, D. V. Gaidarenko, A. G. Leonov, A. A. Panteleev, and A. N. Starostin, Opt. Commun. **105**, 165 (1994).
[6] R. W. Boyd, P. Narum, M. G. Raymer, and D. J. Harter, Phys. Rev. A **24**, 411 (1981).
[7] T. Fu and M. Sargent, III, Opt. Lett. **4**, 366 (1979).
[8] J. F. Valley, G. Khitrova, H. M. Gibbs, J. W. Grantham, and Xu Jiajin, Phys. Rev. Lett. **64**, 2362 (1990).
[9] L. A. Bol'shov, V. V. Likhakskiĭ, and A. P. Napartovich, Zh. Éksp. Teor. Fiz. **72**, 1769 (1977) [Sov. Phys. JETP **45**, 928 (1977)].
[10] L. A. Bol'shov and V. V. Likhanskĭ, Zh. Éksp. Teor. Fiz. **75**, 2047 (1978) [Sov. Phys. JETP **48**, 1030 (1978)].
[11] L. A. Bol'shov, T. K. Kiricheko, and A. P. Favorskĭ, Dokl. Akad. Nauk SSSR **243**, 623 (1978) [Sov. Phys. Dokl. **23**, (1978)].
[12] M. O. Scully and W. E. Lamb, Jr., Phys. Rev. **159**, 208 (1967).
[13] E. V. Baklanov, Zh. Éksp. Teor. Fiz. **65**, 2203 (1973) [Sov. Phys. JETP **38**, 1100 (1973)].
[14] P. Meystre and M. Sargent, III, *Elements of Quantum Optics* (Springer, Berlin, 1990).
[15] B. R. Mollow, Phys. Rev. A **5**, 2217 (1972).
[16] B. R. Mollow, Phys. Rev. **188**, 1969 (1969).
[17] M. Sargent, III, D. A. Holm, and M. S. Zubary, Phys. Rev. A **31**, 3112 (1985).
[18] V. I. Lebedev, *Calculational Processes and Systems*, No. 8 [in Russian] (Nauka, Moscow, 1991).
[19] V. I. Lebedev, *How to Solve Stiff Systems of Differential Equations by Explicit Methods. Numerical Methods and Applications*, ed. by G. I. Marchuk (Boca Raton, 1994).
[20] A. N. Kazakov, V. I. Lebedev, A. A. Medovikov, Russ. J. Num. Anal. Math. Modeling **8**, 47 (1993).
[21] L. Allen and J. H. Eberly, *Optical Resonance and Two-Level Atoms* (Wiley, New York, 1975).
[22] V. I. Bespalov and V. I. Talanov, Pis'ma Zh. Éksp. Teor. Fiz. **3**, 425 (1966) [JETP Lett. **3**, 279 (1966)].
[23] A. Javan and P. L. Kelley, IEEE J. Quant. Electron. **2**, 470 (1966).
[24] D. J. Harter, P. Narum, M. G. Raymer, and R. W. Boyd, Phys. Rev. Lett. **46**, 1192 (1981).
[25] Y. H. Meyer, Opt. Commun. **34**, 439 (1980).
[26] C. H. Skinner and P. D. Kleiber, Phys. Rev. A **21**, 151 (1980).
[27] E. A. Chauchard and Y. H. Meyer, Opt. Commun. **52**, 141 (1994).
[28] I. Golub, G. Erez, and R. Shuker, J. Phys. B **19**, L115 (1986).
[29] A. A. Afanas'ev, V. I. Vaĭchatis, M. V. Ignatavichus, V. I. Kudryashov, Yu. N. Pimenov, and R. V. Yakite, Kvant. Èlektron. **14**, 1689 (1987) [Sov. Phys. Quant. Electron. **17**, 1078 (1987)].
[30] V. I. Vaĭchatis, M. V. Ignatavichus, V. I. Kudryashov, Yu. N. Pimenov, and R. V. Yakite, Kvant. Èlektron. **14**, 762 (1987) [Sov. Phys. Quant. Electron. **17**, 478 (1987)].
[31] A. C. Tam, Phys. Rev. A **19**, 1971 (1979).
[32] D. R. Heathley, E. M. Wright, and G. I. Stegeman, J. Opt. Soc. Am. B **7**, 990 (1990).
[33] G. P. Agrawal, J. Opt. Soc. Am. A **7**, 1072 (1990).
[34] I. I. Vesilova and L. A. Mel'nikov, Opt. Spektrosk. **71**, 175 (1991) [Opt. Spectrosc. **71**, 102 (1991)].
[35] A. A. Mak, L. N. Soms, V. A. Fromzel', and V. E. Yashin, *Neodymium-Glass Lasers* [in Russian] (Nauka, Moscow, 1990).

Translated by Paul F. Schippnick